Research article

Open Access

Involution of the mouse mammary gland is associated with an immune cascade and an acute-phase response, involving LBP, CD14 and STAT3

Torsten Stein[1], Joanna S Morris[1], Claire R Davies[1], Stephen J Weber-Hall[2], Marie-Anne Duffy[1], Victoria J Heath[1], Alexandra K Bell[1], Roderick K Ferrier[1], Gavin P Sandilands[3] and Barry A Gusterson[1]

[1]Division of Cancer Sciences and Molecular Pathology, Western Infirmary, Glasgow, UK
[2]Abbott Laboratories Limited, Diagnostic Division, Maidenhead, Berkshire, UK
[3]Department of Pathology, Western Infirmary, Glasgow, UK

Correspondence: Torsten Stein (e-mail: ts33s@udcf.gla.ac.uk)

Received: 16 Sep 2003 Revisions requested: 12 Nov 2003 Revisions received: 20 Nov 2003 Accepted: 21 Nov 2003 Published: 18 Dec 2003

Breast Cancer Res 2004, **6**:R75-R91 (DOI 10.1186/bcr753)

See related Research article: http://breast-cancer-research.com/content/6/2/R92
and related Commentary: http://breast-cancer-research.com/content/6/2/89

Abstract

Introduction: Involution of the mammary gland is a complex process of controlled apoptosis and tissue remodelling. The aim of the project was to identify genes that are specifically involved in this process.

Methods: We used Affymetrix oligonucleotide microarrays to perform a detailed transcript analysis on the mechanism of controlled involution after withdrawal of the pups at day seven of lactation. Some of the results were confirmed by semi-quantitative reverse transcriptase polymerase chain reaction, Western blotting or immunohistochemistry.

Results: We identified 145 genes that were specifically upregulated during the first 4 days of involution; of these, 49 encoded immunoglobulin genes. A further 12 genes, including those encoding the signal transducer and activator of transcription 3 (*STAT3*), the lipopolysaccharide receptor (*CD14*) and lipopolysaccharide-binding protein (*LBP*), were involved in the acute-phase response, demonstrating that the expression of acute-phase response genes can occur in the mammary gland itself and not only in the liver. Expression of *LBP* and *CD14* was upregulated, at both the RNA and protein level, immediately after pup withdrawal; CD14 was strongly expressed in the luminal epithelial cells. Other genes identified suggested neutrophil activation early in involution, followed by macrophage activation late in the process. Immunohistochemistry and histological staining confirmed the infiltration of the involuting mammary tissue with neutrophils, plasma cells, macrophages and eosinophils.

Conclusion: Oligonucleotide microarrays are a useful tool for identifying genes that are involved in the complex developmental process of mammary gland involution. The genes identified are consistent with an immune cascade, with an early acute-phase response that occurs in the mammary gland itself and resembles a wound healing process.

Keywords: acute-phase response, involution, mammary gland, microarray

Introduction

The mouse mammary gland is an excellent model system with which to study both the regulation of development and the functional differentiation of an organ. Most of the development occurs postnatally, when the gland undergoes a highly regulated cascade of invasive growth, branching, differentiation, secretion, apoptosis and remodelling during each pregnancy cycle [1,2]. Terminal differentiation of the alveolar epithelium is completed at the end of gestation with the onset of milk secretion (lactation).

APR = acute-phase response; C/EBP = CCAAT/enhancer-binding protein; H&E = haematoxylin and eosin; IHC = immunohistochemistry; IL = interleukin; LIF = leukaemia inhibitory factor; LPS = lipopolysaccharide; OSM = oncostatin M; RT–PCR = reverse transcriptase polymerase chain reaction; SOM = self-organising map; TNF = tumour necrosis factor; WAP = whey acidic protein.

After weaning, the entire alveolar epithelium involutes. Involution is reversible within the first 48–72 hours but becomes irreversible thereafter [3]. Apoptosis of the alveolar cells commences within hours of forced weaning, when milk accumulates within the alveolar lumen and the levels of lactogenic hormones decrease. In teat-sealing experiments, Li and colleagues [4] demonstrated that local signals are sufficient to induce apoptosis in alveolar cells and that a continued presence of systemic lactogenic hormones or glucocorticoid injections is unable to block alveolar cell death. During the second, irreversible phase of involution, which is regulated by systemic hormones, the lobuloalveolar architecture is remodelled by proteinase degradation of the basement membrane and the extracellular matrix. The dying cells are finally removed by phagocytosis. Within 2 weeks the gland has returned to a morphological state similar to that of an adult virgin mouse.

Several important genes involved in this involution process have previously been described [5] that operate in specific signalling pathways of remodelling or apoptosis. Our goal was to identify over a defined time course the potential interplay between the processes involved in enforced involution, by studying mRNA expression profiles after withdrawal of the pups at day 7 of lactation. In recent years, oligonucleotide microarray analysis has proved to be a very efficient technique, allowing several thousand genes and expressed sequence tags to be examined in one hybridisation. At the same time, the quality of the arrays and the analysis software have improved dramatically and the applications for this technique have become more and more widespread (see supplement to *Nature Genetics* **32**, December 2002).

Master and colleagues [6] have shown that microarrays are a valuable tool for identifying pathways and cellular processes during the development of mouse mammary gland, when they identified a role for the mouse mammary gland in adaptive thermogenesis during early pup development. We therefore used oligonucleotide microarrays from Affymetrix to investigate the transcriptional expression of about 6000 known genes and another 6000 expressed sequence tags during the first 4 days of mouse mammary gland involution. In this study we identified 145 genes that were specifically upregulated during the first 4 days of involution. These genes illustrated a distinct immune response, resembling a wound healing process, including a primary neutrophil activation and a secondary macrophage activation, a local acute-phase response (APR) and a late B lymphocyte response without any signs of infection. Using F4/80 antibody for immunohistochemistry (IHC) in addition to eosin staining, we showed that infiltration of the mouse mammary tissue by macrophages paralleled the increase of the identified transcripts during involution, and that it was preceded by an activation and increase in the number of neutrophils.

The study further revealed an unexpected infiltration of eosinophils into the mammary tissue during involution. We also showed that the APR protein lipopolysaccharide (LPS)-binding protein (LBP) is not specifically expressed in the liver but in the involuting gland itself, and that CD14 is strongly expressed in the luminal epithelial cells during involution. We discuss a model of how LBP and CD14 might be involved in the clearance of the gland and how neutrophils and macrophages could be activated during the first 4 days of involution.

Materials and methods

RNA isolation

All animal work was conducted in accordance with accepted standards of humane animal care, was in compliance with the Helsinki Declaration and was approved by an ethical committee. We used the fourth (inguinal) mammary gland from three individual Balb/C mice per time point from one flank. As morphological controls we used the corresponding gland from the other side to generate whole mounts. The mice were mated at 12 weeks of age to make sure that the glands were fully developed. The glands were harvested at the following developmental stages: virgin, 10 and 12 weeks; pregnancy days 1, 2, 3, 8.5, 12.5, 14.5 and 17.5; lactation days 1, 3 and 7; and involution days 1, 2, 3, 4 and 20. For involution samples, the pups were force-weaned after 7 days of lactation. The lymph node within the gland was removed, the gland was snap-frozen in liquid nitrogen and kept at –80°C until further extraction. The glands were homogenised in a dismembrator (B Braun Biotech, Melsungen, Germany) and were immediately treated with Trizol reagent (Invitrogen, Paisley, UK). Total RNA was extracted in accordance with the manufacturer's protocol and eluted in nuclease-free water. Small RNA fragments were removed by further purification with RNeasy-mini columns (Qiagen, Hilden, Germany) in accordance with the manufacturer's protocol. The RNA was quantified by spectrophotometer and the quality was tested on an Agilent (Palo Alto, CA, USA) bioanalyser.

Oligonucleotide microarray hybridisation

Total RNA (10 μg) from each time point was used for the production of biotinylated cRNA as described in the Affymetrix (High Wycombe, UK) manual. The quality of the labelled cRNA was confirmed by hybridisation to an Affymetrix test chip (Test3-chip). All experiments were performed in triplicate with RNA from three individual mice. Labelled cRNA (15 μg) was hybridised to the MG-U74Av2 chip from Affymetrix for 16 hours at 45°C in a rotating hybridisation oven. After washing and staining of the chip in an Affymetrix-Fluidic station, the chip was scanned in an Agilent scanner and the raw data were analysed by the Microarray Suite 5.0 software. All results were scaled to a target signal of 100. The scaling factors of the individual experiments did not differ more than threefold between

each other. Results from 12,488 probe sets were collected (see Additional file 1).

Data analysis

Details of the algorithms of the software are available at http://www.Affymetrix.com. The data were included in a database, constructed with Affymetrix MicroDB® software, and analysed with the Affymetrix Data Mining Tool® (DMT). For SOM (self-organising map) cluster analysis, the expression profiles were prefiltered for a relative difference of more than 1.8-fold and an absolute difference greater than 33 between the lowest and highest expression signals. The filter for the lowest signal was set to 20 and that for the highest signal to 20,000. Initialisation was performed with random vectors, and a Gaussian neighbourhood was selected.

In a first selection, the results of the probe sets showing at least three signals with $P \leq 0.04$ or below were combined to 'virgin' (v10, v12), 'early pregnancy' (P1, P2, P3), 'mid–late pregnancy' (P8.5, P12.5, P14.5, P17.5), 'lactation' (Lac1, Lac2 Lac3), 'early involution' (Inv1, Inv2), 'mid-involution' (Inv3, Inv4) and 'late involution' (Inv20). Ten separate SOM clustering analyses were performed (3 × 4) and only those probe sets that were always in an early- or mid-involution specific cluster were considered for further analyses (488 probe sets). For downregulated genes, only those probe sets that were always in a cluster showing only downregulation at involution were considered for further analysis (144 probe sets). Probe sets showing upregulation were then used for another round of 10 SOM clustering analyses (4 × 5), but this time as individual time points. Those clusters, which showed their highest expression either at Inv1, Inv2, Inv3 or Inv4 and showed no upregulation at earlier time points, were combined (379 probe sets).

For direct comparison of two time points, each of the three experiments from one time point (Inv1, Inv2, Inv3 or Inv4) was compared with each of the three experiments from lactation day 7 used as baseline, to produce a total of nine comparisons. Only probe sets that produced at least eight out of nine change values of $P \leq 0.0024$ (or $P \geq 0.9976$ for decrease) and for which all three signals of the particular involution time point had a detection $P \leq 0.04$ were considered as being increased.

The degree of change between two time points is described as the log ratio (2^x) and reflects the average of the nine comparisons. Only probe sets showing a log ratio of at least 0.84 (1.8-fold) were selected (1044 probe sets increased, 461 probe sets decreased). A combination of the direct comparison result and the SOM clustering resulted in 220 probe sets (21% of increased probe sets; 58% of probe sets identified through SOM clustering) for upregulated genes and 44 probe sets (9.5% of decreased probe sets; 30.5% of probe sets identified through SOM clustering) for downregulated genes. Each of these was again checked individually for involution-specific upregulation or downregulation. The final selections of 152 probe sets (14.5% of increased probe sets; 40% of probe sets identified through SOM clustering) showing upregulation and 16 probe sets (3.5% of decreased probe sets; 11.1% of probe sets identified through SOM clustering) showing downregulation reflected those which fitted this criterion best (see Additional file 2). The 152 probe sets were divided into immunoglobulin-encoding genes (49 genes) and other genes and were further clustered by a Pearson correlation clustering method, by using GeneSpring® (Silicon Genetics, Redwood City, CA, USA).

Protein extracts and Western blotting

Protein extracts were made from 2–3 mm strips of the fourth inguinal mammary gland between lymph node and body and extracted in lysis buffer (50 mM Tris-HCl, 150 mM NaCl, 5 mM EDTA, 0.5% Triton X-100, 50 mM NaF plus protease inhibitor mix). The glands were homogenised with a plastic homogeniser in a 1.5 ml tube, incubated for 10 min at 4°C and centrifuged for 10 min at 20,000*g* at 4°C. The protein extracts (supernatant, 25 μg) were separated on a 4–12% NuPage gel (Invitrogen) in MES buffer under denaturing and reducing conditions. The protein was transferred onto nitrocellulose membrane (Schleicher and Schuell, Dassel, Germany) and the proteins were detected by enhanced chemiluminescence with Amersham ECL®.

The antibodies used were anti-LBP (N-17; dilution 1 : 500; Santa Cruz Biotechnology, Santa Cruz, CA, USA), anti-(mouse CD14) (M-20; dilution 1 : 500; Santa Cruz Biotechnology), and anti-(mouse β-actin) (ab205; dilution 1 : 8000; Abcam, Cambridge, UK).

Immunohistochemistry

The antibodies were used at the following dilutions: 1 : 500 biotinylated rat anti-(mouse B220) (RA3-6B2; BD Biosciences-Pharmingen, San Diego, CA, USA), 1 : 40 goat anti-(mouse CD14) (M-20; Santa Cruz) and 1 : 50 rat anti-(mouse F4/80) (gift from JW Pollard). Paraffin-embedded tissue sections were stained by using the three-step streptavidin–biotin system incorporating antigen retrieval by digestion for 10 min with 0.02% trypsin. Endogenous biotin was blocked with an avidin–biotin blocking system (Vector Labs, Burlingame, CA, USA) and Fcγ receptors were pre-blocked with 10% normal rabbit serum. Binding of streptavidin–biotin-conjugated horseradish peroxidase was visualised by using 3,3′-diaminobenzidine tetrahydrochloride. Sections were counterstained with haematoxylin and eosin (H&E). A fluorescein isothiocyanate-labelled neutrophil-specific antibody (7/4; Caltag, Burlingame, CA, USA) was used for immunofluorescent staining of frozen mammary tissue at 1 : 50 dilution.

Staining with methyl green and pyronin

Paraffin sections were dewaxed and rehydrated, then rinsed in pH 4.8 buffer (0.08 M acetic acid, 0.12 M sodium acetate) and stained for 25 min in methyl green/pyronin solution (9 ml of 2% aqueous methyl green CI 42590, 4 ml of 2% aqueous pyronin Y, 23 ml of acetate buffer, pH 4.8, and 14 ml of glycerol). Sections were again rinsed in pH 4.8 buffer, followed by acetone/xylene (1 : 1). Finally they were dehydrated, cleared and mounted.

Reverse transcriptase polymerase chain reaction (RT–PCR)

Total RNA (10 µg) was treated with DNase (DNA-free™; Invitrogen) in accordance with the manufacturer's protocol and resuspended in 100 µl of nuclease-free water. A 10 µl portion of this solution was used to produce cDNA, using SuperscriptII (Invitrogen) in accordance with the manufacturer's protocol. This cDNA (1 µl) was used in each PCR reaction with Hot-Star *Taq* polymerase (Qiagen). An Eppendorf Mastercycler gradient was used for the chain reaction, with 25–35 PCR cycles (30 s at 90°C, 30 s at 55–59°C, 30 s at 72°C). The following oligonucleotides were used: *GRO1*, 5′-ACCGAAGTCATAGCCACACTC-3′ and 5′-TTGACACTTAGTGGTCTCCCA-3′; *LRG*, 5′-CAGCATCAAGGAAGCCTCCA-3′ and 5′-TTGGCCGAG-GTGCTGAAC-3′; *BMAC*, 5′-CGAGGAGAAGATGGT-TATCGTC-3′ and 5′-AGCATCAGCCTCCTTTGTGA-3′; *CD68*, 5′-CAGCACAGTGGACATTCATG-3′ and 5′-GG-TAACTGTTGAGTCAGTGGC-3′; *β-actin*, 5′-T(C/T)GTG-ATGGACTCCGG(A/T)GAC-3′ and 5′-C(G/A)CCAGAC-AGCACTGTGTTG-3′.

Results

To identify genes that were solely upregulated or downregulated during involution of the mouse mammary gland, we performed an oligonucleotide microarray analysis on total RNA from all developmental stages of an adult virgin mammary gland as outlined in the Materials and methods section.

We first tested for random variation between experiments by comparing RNA expression signals of two individual glands from the same mouse during mid-pregnancy (day 11.5) with Affymetrix Microarray Suite 5.0 (data not shown). The two arrays showed fewer than 1% changes that were more than twofold (log ratio 1), which was in the expected range of the Affymetrix arrays. Because RNA samples were taken in triplicate for each time point and each sample of lactation day 7 was cross-compared against each of the samples of the involution time points to identify upregulated or downregulated genes (nine comparisons per involution time point), random variation was reduced even further.

As controls, known gene expression profiles, including those for the milk protein genes *casein* α, β, γ, δ, κ and *butyrophilin*, were tested for correct expression. They all showed the expected upregulation during mid-pregnancy and downregulation at the onset of involution, and, for *casein* δ, upregulation at parturition (Fig. 1a). Further control genes with lower expression levels included those encoding the transcription factors msh-like 2 (*MSX2*), LIM domain only 4 (*LMO4*) and Bcl2-associated X-protein (*BAX*), which showed the expected upregulation during early and mid-pregnancy, and early involution respectively (Fig. 1b–d).

Figure 1

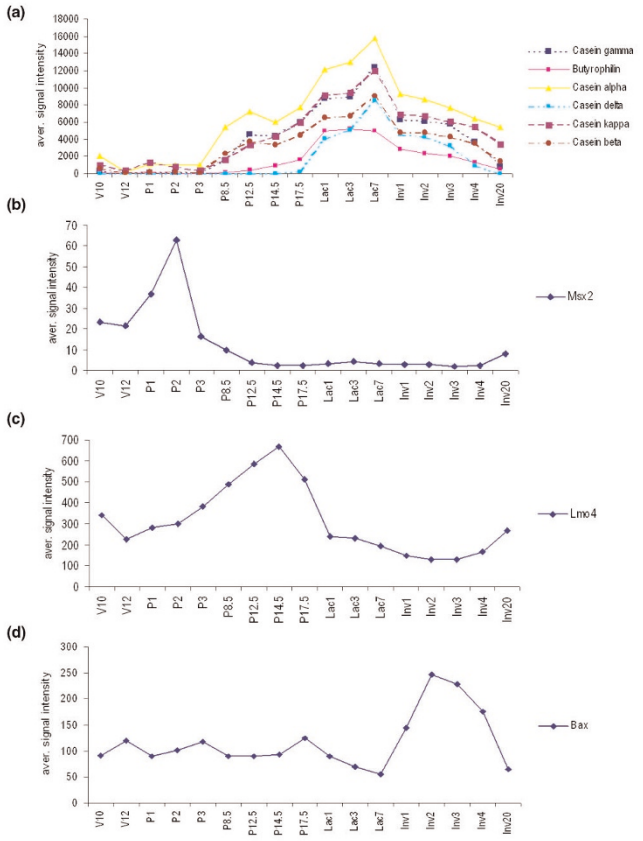

RNA expression profiles of selected control genes. The graphs show the scaled average signals (*y*-axis) for the milk protein genes *casein* α, β, γ, δ, κ and *butyrophilin* **(a)**, as well as the transcription factor genes *MSX2* **(b)** and *LMO4* **(c)**, and the pro-apoptotic gene *BAX* **(d)** at the different stages of adult mouse mammary gland development (*x*-axis).

Genes specific for involution

Having demonstrated that our controls showed the expected expression profiles, we went on to identify those genes that were specifically upregulated or downregulated during involution, using the criteria and procedures outlined in the Materials and methods section. We identified 152 probe sets, representing 145 genes (7 probe sets were redundant), that were specifically upregulated at least 1.8-fold (log ratio 0.84) after pup withdrawal (Tables 1 and 2), but only 16 probe sets that were specifically downregulated (Table 3). Of the 152 probe sets

Table 1

List of involution-specific genes clustered with the use of Pearson correlation clustering

DMT probe set	Log ratio	Gene description
Cluster 1		
100034_at	3.42	Maspin
102712_at	3.27	Serum amyloid A3
98041_at	8.01	Ribonuclease 1, pancreatic
96056_at	1.42	RhoC
160686_at	2.07	Hypothetical transcription factor
101996_at	1.53	Protein tyrosine phosphatase, non-receptor type 2
95462_at	2.11	HFB2 homologue
99633_at	1.65	Neurochondrin-1
101892_f_at	0.86	Fused toes
104340_at	1.4	Methyl-CpG binding protein, MBD1
99582_at	1.27	Tumour-associated calcium signal transducer 1
103059_at	1.44	MAT8, FXYD domain-containing ion-transport regulator 3
101583_at	0.89	B-cell translocation gene 2, anti-proliferative
100893_at	1.6	Serine palmitoyltransferase, long chain base subunit 2
96657_at	1.81	Spermidine/spermine N^1-acetyl transferase
93017_at	2.16	Syntenin
104725_at	2	Small ras-like GTPase Tc10
93220_at	2.33	Procollagen, type IV, α 5
101995_at	1.59	Sequestosome 1
160713_at	2.71	Arsenite inducible RNA-associated protein (Airap)
95674_r_at	2.71	Brain-abundant membrane-attached signal protein 1
160894_at	2.48	CCAAT/enhancer binding protein (C/EBP), δ
95673_s_at	6.11	Brain-abundant membrane-attached signal protein 1
104701_at	2.42	Basic helix–loop–helix protein B2/DEC1
Cluster 2		
95746_at	1.34	ATPase, H^+ transporting, lysosomal (vacuolar proton pump), α 70 kDa, isoform 1
97492_at	1.41	Hypothetical protein with thioredoxin domain
94850_at	1.17	Acyl-coenzyme A thioesterase 3, mitochondrial
95622_at	1	Host cell factor homologue
101410_at	2.96	Claudin 4/mCPE receptor
160106_at	1.73	Capping protein (actin filament), gelsolin-like
103305_at	3.52	Integrin β_4
98151_s_at	1.06	Catenin Src
93347_at	0.88	RAB24, member of Ras oncogene family
Cluster 3		
102761_at	1.47	GrpE-like 2, mitochondrial
162011_f_at	1.15	Ras homologue gene family, member U
96747_at	1.16	Ras homologue gene family, member U
103065_at	1.66	Solute carrier family 20, member 1
93435_at	8.41	Cytochrome P450, 24
95348_at	2.27	GRO1 chemokine (C-X-C motif) ligand 1, GRO1/CXCL1
95745_g_at	1.33	ATPase, H^+ transporting, lysosomal (vacuolar proton pump), alpha 70kDa, isoform 1
94734_at	4.14	α_1-acid glycoprotein 2, orosomucoid 2
92312_at	1.33	Phosphatidylinositol 3-kinase p170
98910_at	0.84	Homology to ETS-domain protein ELK-1 from rat
161139_f_at	1.8	DDEF1/development and differentiation enhancing 1
Cluster 4		
100136_at	1.15	Lysosomal membrane glycoprotein 2
101055_at	1.11	Protective protein for β-galactosidase
103812_at	3.31	Chloride channel calcium activated 1
101389_at	1.93	scavenger receptor class B, member 2
93728_at	2.73	Transforming growth factor β_1 induced transcript 4, TSC-22
101587_at	4.37	Microsomal epoxide hydrolase (Eph1), allele b
96119_s_at	3.32	Angiopoietin-like 4
97420_at	4.04	Leucine-rich α_2-glycoprotein
102114_f_at	3.7	Angiopoietin-like 4/fasting-induced adipose factor FIAF
Cluster 5		
100513_at	2.39	DDEF1/development and differentiation enhancing
93281_at	0.89	Taipoxin-associated calcium-binding protein 49 mRNA, reticulocalbin2
96738_at	1.61	Metalloprotease/disintegrin/cysteine-rich protein precursor (MDC9)
100565_at	1.95	Glucosamine-6-phosphate deaminase
103503_at	2.06	Phospholipase $C\gamma_2$ (phosphatidylinositol-specific)
160127_at	1.01	Cyclin G_1
97948_at	3.39	Retinoblastoma 1
Cluster 6		
162479_f_at	0.89	Ferritin light chain 1
97529_at	3.12	Annexin 8

Continued overleaf

Table 1 *continued*

List of involution-specific genes clustered with the use of Pearson correlation clustering

DMT probe set	Log ratio	Gene description
Cluster 7		
102255_at	3.41	Oncostatin M receptor
162206_f_at	3.85	Suppressor of cytokine signalling 3
104155_f_at	1.79	ATF3 (LRG-21)
93294_at	4.31	Fibroblast inducible secreted protein, connective tissue growth factor
102362_i_at	3.57	JunB
93536_at	1.61	Bcl2-associated X protein
103448_at	1.31	S100 calcium binding protein A8 (calgranulin A)
95680_at	1.22	Protein phosphatase 1, regulatory (inhibitor) subunit 2
96953_at	1.49	Small inducible cytokine subfamily B (Cys-X-Cys), member 14 /BMAC
99952_at	7.05	Chitinase 3-like 1
95681_f_at	2.09	Protein phosphatase 1, regulatory (inhibitor) subunit 2
Cluster 8		
100313_at	1.54	Integrin α_8
101306_f_at	3.34	Serum amyloid A pseudogene
100333_at	2.34	Serum amyloid A2 (SAA-2)
96123_at	1.69	LPS-binding protein
96766_s_at	2.2	Receptor tyrosine kinase, Tyro3
96940_at	0.99	TEA-domain family member 2
100491_at	0.84	Solute carrier family 16 (monocarbox. acid transporters), member 2
96592_at	2.39	Phosphatidylinositol 3-kinase, reg. subunit, polypeptide 1 (p85α)
Cluster 8 (continued)		
99133_at	1.65	Solute carrier family 3 (activators of dibasic and neutral amino acid transport), member 2
102049_at	4.25	Pyruvate dehydrogenase kinase, isoenzyme 4
94881_at	3.49	Cyclin-dependent kinase inhibitor 1A (p21)
161650_at	1.94	Secretory leukoprotease inhibitor
92858_at	4.89	Secretory leukoprotease inhibitor
96614_at	1.67	Hypothetical protein
101963_at	1.61	Cathepsin L
92851_at	2.06	Caeruloplasmin
93753_at	1.58	LPS-induced TN factor
98088_at	2.6	CD14 antigen
101287_s_at	4.71	Cytochrome P450, 2d11
94384_at	1.28	Immediate early response 3
99099_at	0.93	Acute-phase response factor APRF/STAT3
102751_at	1.9	Transforming growth factor, β_3
102313_at	1.15	GTP cyclohydrolase 1
Cluster 9		
96679_at	1.25	DnaJ (Hsp40) homologue, subfamily B, member 9
Cluster 10		
103016_s_at	2.77	CD68 antigen
95706_at	4.15	Galectin 3
98543_at	2.69	Cathepsin S
99071_at	1.42	Macrophage-expressed gene 1, Mpeg1/MPS1
104023_at	1.2	Immunoglobulin superfamily, member 7
93318_at	2.59	Adhesion molecule ninjurin

The genes are listed in their order of appearance in the gene tree after Pearson correlation clustering. The DMT probe set number refers to the number of the probe on the Affymetrix MG-U74Av2 chip. The log ratio describes the average change of signal intensity between lactation day 7 and the day of highest expression during involution, on a $\log_2$ scale. The gene description refers to the description of the probe set on the NetAffx website.

identified, 49 targeted immunoglobulins (Table 2). The expression profiles of the other 103 probe sets (Table 1) were clustered further with the Pearson correlation clustering function in GeneSpring® to identify genes that were expressed either early or late after pup removal (Fig. 2a). The resulting gene tree was then grouped into 10 clusters of similarly expressed genes.

Clusters 1, 2, 3 and 5 contained 46 genes that were all characterised by their strongest expression on the first day after forced weaning. Whereas cluster 1 showed a constant baseline expression over all the other developmental stages, genes in cluster 2 were additionally downregulated during lactation, and genes in cluster 5 decreased over the time course towards lactation day 7. Cluster 3 was of specific interest because it contained genes that were upregulated only on the very first day after weaning and were strongly downregulated on the second day. The genes in these four clusters were therefore likely to be involved in the immediate early events during the switch from lactation to involution; six of them encode transcriptional regulatory proteins. Genes in cluster 4 were also upregulated on the first day, but their expression peaked on day 2 of involution and declined thereafter. They are therefore likely to be involved in secondary events during the reversible stage of involution.

Table 2

List of genes downregulated during involution

DMT probe set	Log ratio	Gene description
101580_at	−1.1	Cytochrome *c* oxidase subunit VIIb
92587_at	−1.41	Ferredoxin 1
160091_at	−1.14	Phosphoglycerate mutase 1
160385_at	−1.24	RIKEN cDNA 5730591C18 gene (hypothetical mitochondrial)
160184_at	−1.26	RIKEN cDNA 1200007D18 gene
162077_f_at	−2.04	Stearoyl-coenzyme A desaturase 2
93332_at	−1.36	CD36 antigen
95611_at	−1.82	Lipoprotein lipase
94966_at	−1.11	Glucose-6-phosphate dehydrogenase X-linked
95053_s_at	−0.91	Succinate dehydrogenase complex, subunit B, iron sulphur (Ip) putative orthologue
99618_at	−1.14	Homologous to ubiquinol–cytochrome *c* reductase complex 6.4 kDa protein (complex III subunit XI)
93308_s_at	−2.03	Pyruvate carboxylase
98575_at	−2.24	Fatty acid synthase
94427_at	−0.91	Coatomer protein complex, subunit γ_1
96850_at	−0.95	Eukaryotic translation initiation factor 4 γ, 3, putative orthologue
99009_at	−0.91	Nicotinamide nucleotide transhydrogenase

For notes, see footnote to Table 1.

Cluster 6 represented only two genes. Both showed a strong upregulation on the first day and remained highly expressed even 20 days after weaning, suggesting that they might be important over the whole period of involution. Cluster 7, which included the pro-apoptotic factor gene *BAX*, contained genes whose transcript level increased on the first day but increased further towards day 3 of involution. Genes in cluster 8 remained highly expressed between the first and third day of involution, after which they returned to baseline levels. This cluster included the transcription factor gene *STAT3/APRF* or *acute-phase response factor*. Cluster 9 contained only a single gene, *DnaJ [Hsp40] homologue, subfamily B, member 9*, coding for a mitochondrial stress protein. This gene has a unique expression profile in that it was upregulated on the second day after weaning and declined strongly after day 3. The genes in cluster 10 were expressed strongest late in involution (day 4) and therefore seem to represent genes that are needed only for the second stage of involution.

Only 16 genes were specifically downregulated during involution. Their transcript levels decreased on the first day after weaning (Fig. 2b) and 11 of them encoded metabolic or respiratory proteins. No anti-apoptotic or cell survival genes were specifically downregulated during this involution stage.

Figure 2

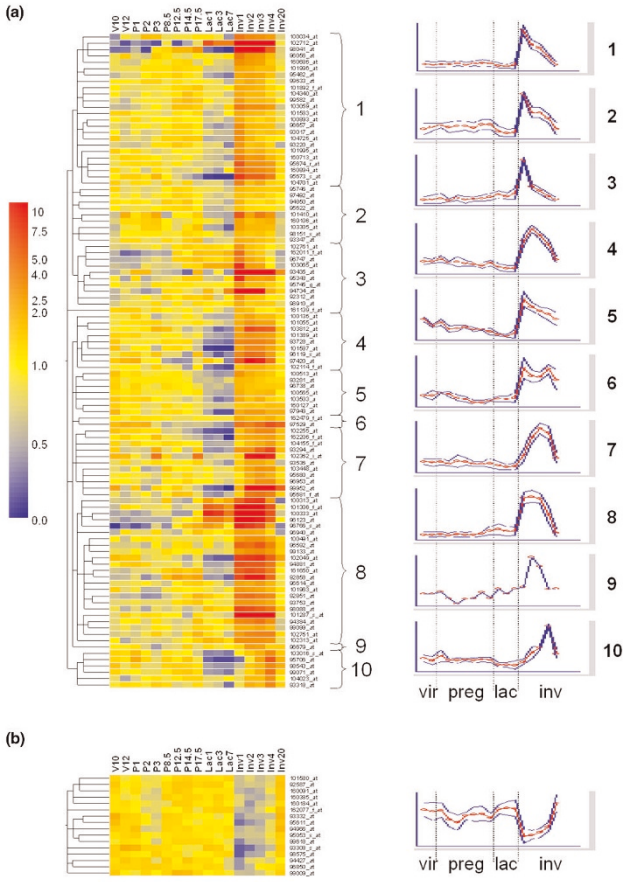

Pearson correlation clustering of involution specific genes. **(a)** One hundred and three upregulated probe sets identified through SOM clustering were clustered with the Pearson correlation clustering program of GeneSpring (Silicon Genetics). The colours (see colour bar) represent a relative measure for the expression, with 1 representing the median, the red colour upregulated and blue downregulated gene expression. The resulting gene tree was grouped into 10 clusters of similarly expressed genes (shown bracketed at the right) and their average expression patterns are shown on the right as graphs (red lines) with standard deviations (blue lines) (DMT®; Affymetrix). Note that the *y*-axes represent only arbitrary expression levels and are not scaled identically between graphs. **(b)** Sixteen downregulated genes were clustered by using the software mentioned above and their average expression (red line) and standard deviations (blue lines) are shown in the graph on the right (DMT®; Affymetrix). Abbreviations: vir, virgin; preg, pregnancy; lac, lactation; inv, involution.

A distinct lymphocytic response during the second stage of involution

The 49 immunoglobulin genes identified showed a very similar expression pattern (Fig. 3a). RNA levels increased

Table 3

List of immunoglobulin genes upregulated at involution

DMT probe set	Log ratio	Gene description
100299_f_at	1.34	Igκ chain variable 8 (V8)
101331_f_at	1.86	Igκ chain variable 8 (V8)
102372_at	1.69	Immunoglobulin joining chain
161486_f_at	1.12	Immunoglobulin heavy chain (J558 family)
96964_at	1.1	Ig light chain V-region CC83 rearranged gene, exons 1 and 2
93638_s_at	4.28	Immunoglobulin lambda chain, variable 1
100322_at	1.37	Immunoglobulin heavy chain 4 (serum IgG1)
100362_f_at	1.97	Germline immunoglobulin V(H)II gene H8
100376_f_at	2.11	Clone BHS2.19 immunoglobulin heavy chain variable region precursor
97563_f_at	1.71	Ig heavy chain gene, CDR3 region
101320_f_at	1.14	Ig B cell antigen receptor gene
101319_f_at	1.36	Ig B cell antigen receptor gene
98765_f_at	1.57	Immunoglobulin heavy chain (J558 family)
100360_f_at	1.7	Immunoglobulin heavy chain 4 (serum IgG1)
101718_f_at	1.65	Igκ chain variable 8 (V8)
97567_f_at	1.64	Igκ chain variable 8 (V8)
101640_f_at	1.75	Igκ chain variable 8 (V8)
96972_f_at	1.61	Igκ chain variable 8 (V8)
97566_f_at	1.66	Igκ chain variable 8 (V8)
101751_f_at	1.62	B-cell receptor
96971_f_at	1.91	Igκ light chain V-Jκ 5 joining region (cell line CH2)
102585_f_at	1.61	Igκ chain variable 8 (V8)
99369_f_at	1.6	Igκ light chain variable region precursor (Vk10c) gene
100721_f_at	1.46	Recombinant antineuraminidase single chain Ig VH and VL domains
101752_f_at	1.75	Immunoglobulin heavy chain 4 (serum IgG1)
102076_at	1.13	IgVκ aj4
100682_f_at	1.73	Igκ chain variable 8 (V8)
97575_f_at	1.64	Clone BHS3.26 immunoglobulin heavy chain variable region precursor
93927_f_at	2.53	Immunoglobulin heavy chain 4 (serum IgG1)
97577_f_at	1.55	Immunoglobulin heavy chain 6 (heavy chain of IgM)
97576_f_at	2.47	Immunoglobulin heavy chain 4 (serum IgG1)
97008_f_at	2.27	Clone CPS1.13 germline Ig variable region heavy chain precursor pseudogene
101747_f_at	1.79	(3C10) IgA V-D-J heavy chain
101871_f_at	2.28	Immunoglobulin heavy chain 4 (serum IgG1)
97574_f_at	2.34	Immunoglobulin heavy chain (J558 family)
101745_f_at	1.13	Immunoglobulin heavy chain 6 (heavy chain of IgM)
101720_f_at	1.75	Igκ chain variable 8 (V8)
97009_f_at	2.48	Immunoglobulin heavy chain variable region
102154_f_at	2.1	Igκ chain variable 8 (V8)
102155_f_at	1.09	Ig aberrantly rearranged κ-chain V10-J2 gene (Vκ-21 subfamily) from plasmacytoma 3386
102157_f_at	1.73	Igκ chain variable 8 (V8)
92470_f_at	1.54	Immunoglobulin heavy chain (J558 family)
94725_f_at	1.67	Variable light chain
93904_f_at	2.18	Clone N1.1.b immunoglobulin heavy chain VDJ region gene
96973_f_at	1.98	Ig V(H)II gene H18
101656_f_at	2.28	Igκ chain variable 5 (V5 family)
97564_f_at	2.37	Igκ light chain variable region
96975_at	1.7	Ig Vκ-PCG-4 gene

 For notes, see footnote to Table 1.

Figure 3

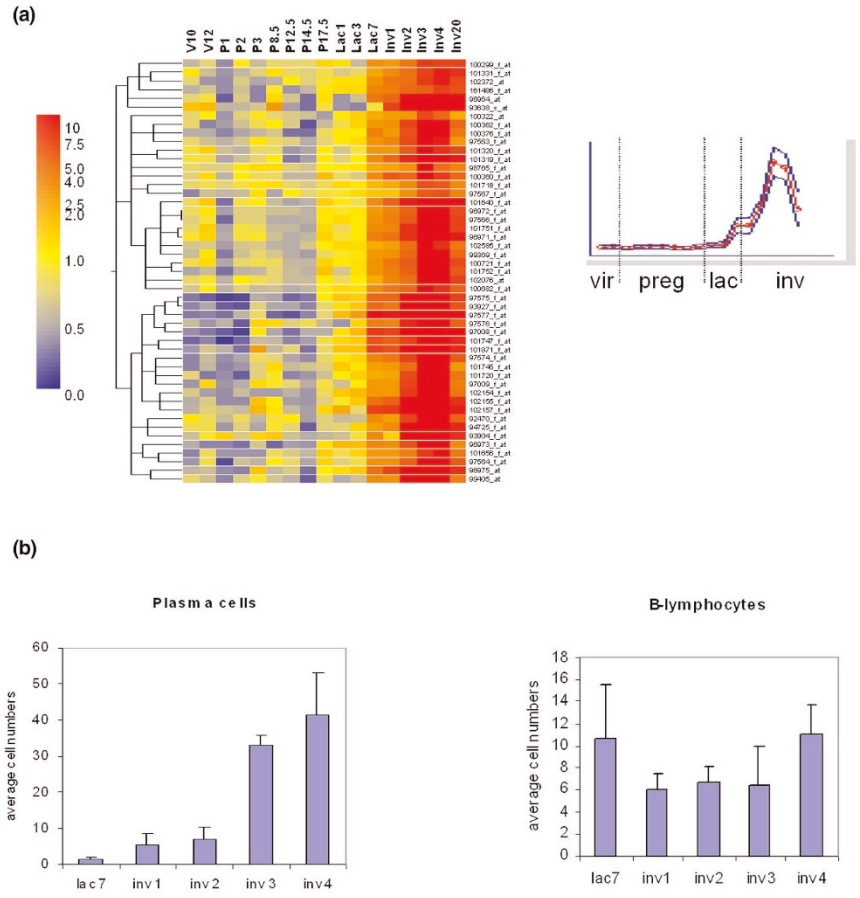

B-lymphocyte response during involution. **(a)** Pearson correlation clustering of immunoglobulin genes. The colours (see colour bar) represent a relative measure for the expression level, with 1 representing the median. Forty-nine immunoglobulin genes that were upregulated during involution were clustered by using the Pearson correlation clustering function from GeneSpring (Silicon Genetics); their average expression (red line) and standard deviations (blue lines) are shown in the graph on the right (DMT®; Affymetrix). Note that the *y*-axis represents only an arbitrary level of expression. Abbreviations: vir, virgin; preg, pregnancy; lac, lactation; inv, involution. **(b)** Cell count of plasma cells and B220$^+$ B lymphocyes present in the mammary tissue during involution. Tissue sections were stained either with methyl green and pyronin or with an antibody against CD45R, and plasma cells and B lymphocytes were counted. Cell counts were taken from 20 high-power fields from each section in triplicate from three individual mice.

slightly on day 7 of lactation, and this expression rate remained the same on the first day of involution, but a second, much stronger response was found between the second day and fourth day after pup removal. By day 20 of involution, expression of these genes had decreased, but in 37 cases expression levels were still higher than in 12-week-old virgin mice. This finding pointed strongly towards a B-cell response induced by enforced weaning. To determine whether this upregulation was due to an increased infiltration of B lymphocytes or plasma cells, or merely reflected an increased transcriptional activity of cells that were already present in the mammary tissue, we performed IHC with antibodies against the B cell marker B-220. The intra-mammary lymph node served as an internal positive control.

Plasma cells were identified in H&E-stained sections by their characteristic shape, nuclear characteristics, clear Golgi region and amphiphilic cytoplasm. They were confirmed by staining with methyl green and pyronin. To count the number of cells per unit area, standard histological methods were used: 20 high-power fields were randomly selected with the section out of the plane of focus to remove observer bias. Sections were then focused and cells were counted. In all cases a section from each of three individual mice was examined. The mean of the three readings is recorded, together with the standard error (Fig. 3a). There was a marked increase in plasma cells on days 3 and 4. The intra-mammary lymph node had large numbers of maturing plasma cells, which were migrating from the hilum into the surrounding mammary tissue. All

measurements were therefore taken at a distance from the region of the lymph node. In contrast with the plasma cells, the number of B-220$^+$ B lymphocytes showed no obvious change (Fig. 3a).

Involution-specific genes describe a coordinated early activation of neutrophils and late activation of macrophages and eosinophils

On the basis of the finding of a plasma cell response during involution, we looked for further indications of an immune response. Although infiltration of immune cells, including neutrophils and macrophages, into the mammary gland has been reported for many animals during involution, this infiltration has not yet been shown for mice, rats or humans. Further, it is so far largely unknown what attracts these leukocytes to the mammary gland during involution. We therefore investigated whether any of our identified genes were involved in neutrophil or macrophage activation. We found that the neutrophil-attracting chemokine encoded by *growth-related oncogene 1* (*GRO1*/*CXCL1*/*KC*) was induced on the very first day of involution, followed by an increased expression of the neutrophilic granulocyte marker encoded by *leucine-rich* α_2*-glycoprotein* (*LRG*) during the first and second days (Fig. 4a). In contrast, the expression of the gene *small inducible cytokine subfamily B* (*C-X-C*) *member 14* (*CXCL14*/*BMAC*), encoding the B-cell and macrophage-attracting chemokine (Fig. 4b), and of the macrophage-expressed *chitinase 3-like1*, was delayed during involution and peaked only on the third day (cluster 7). In addition, RNA levels of genes associated with macrophage differentiation, including *CD68* (Fig. 4b), *cathepsin S*, *galectin 3* and *macrophage-expressed gene Mpeg1*/*MPS1* increased on days 3 and 4 of involution (cluster 10).

To verify these results we performed semi-quantitative RT–PCR for *GRO1*, *LRG*, *CXCL14*/*BMAC* and *CD68*, which confirmed our microarray data (Fig. 4c). The expression profiles of our identified genes therefore described a scenario in which forced weaning induces *GRO1* expression and an early influx of neutrophils, followed by the expression of *CXCL14*/*BMAC* and the activation of macrophages. The gene encoding another major chemokine for the recruitment and regulation of macrophages, colony-stimulating factor 1 (*CSF1*), together with that of its receptor, *CSF1R*, also showed increased expression during involution, peaking on day 4 of involution (data not shown). However, their expression profiles were not specific for the involution process and showed additional upregulation in virgin mice and during early pregnancy.

To examine whether the increase in RNA levels was also reflected in the number of neutrophils and macrophages present in the mammary tissue, we stained three mammary gland sections from three individual mice by IHC for the macrophage marker F4/80 and counterstained with H&E. Neutrophils were identified through their polymorphonuclear morphology, clear cytoplasm and only weak staining with eosin (Fig. 4d). Their presence in the mammary gland was confirmed with a fluorescein isothiocyanate-labelled neutrophil-specific antibody on frozen mammary tissue (data not shown). Neutrophils and macrophages were counted from 20 and 50 high-power fields, respectively, for each tissue section. Whereas the number of neutrophils increased on the first day, decreased slightly on the second day and increased again on days 3 and 4, the number of macrophages only increased markedly on the fourth day, as could be seen by staining with F4/80 antibody (Fig. 4e). However, macrophage numbers in the surrounding connective tissue increased already on day 3 of involution (data not shown). In addition, we found a strong increase in the number of eosinophils in the mammary tissue on day 4 of involution. This cell type was identified by its strong staining by eosin and its polymorphonuclear morphology, and could be distinguished from neutrophils by its staining with the F4/80 antibody and its granular cytoplasm (Fig. 4d).

The involuting mammary gland shows an early APR

The transcription factor *STAT3*/*APRF* is a key component of the involution process but is also strongly involved in the APR as part of the innate immune system. We therefore asked whether any known STAT3 target genes or members of the APR pathway were specifically upregulated during involution.

Of the identified 96 genes, 12 were either directly associated with the APR or have been shown to be inducible by LPS (Table 4). These included the transcription factor gene *STAT3* itself, whose RNA level was upregulated nearly twofold on the first day of involution and remained at that level of expression until day 3, after which it dropped back to pre-involution levels. Five of the genes associated with the APR pathway showed a similar expression profile and were therefore grouped together with *STAT3* in cluster 8, including the genes *LPS-binding protein* (*LBP*) and the LPS receptor *CD14*. These two genes increased approximately threefold and sixfold respectively (log ratios 1.69 and 2.6). Other LPS-induced APR genes included in cluster 8 were *serum amyloid A2* and *serum amyloid pseudogene*, *caeruloplasmin*, the gene encoding the anti-inflammatory whey acidic protein (WAP)-domain protein *secretory leukoprotease inhibitor* (*SLPI*), and the transcription factor gene *LPS-induced TNF-*α *factor* (*LITAF*). The *immediate early response 3* gene, found in cluster 8, has a LPS-induced human orthologue, *differentiation-dependent gene 2* (*DIF2*), and was therefore included in this list. Further genes of the APR pathway, namely *CCAAT/enhancer-binding protein* δ (*C/EBP*δ) and *serum amyloid A3*, grouped together in cluster 1, whereas α_1*-acid glycoprotein 2* (*orosomucoid 2*) was upregulated only on the first day of involution. The

Figure 4

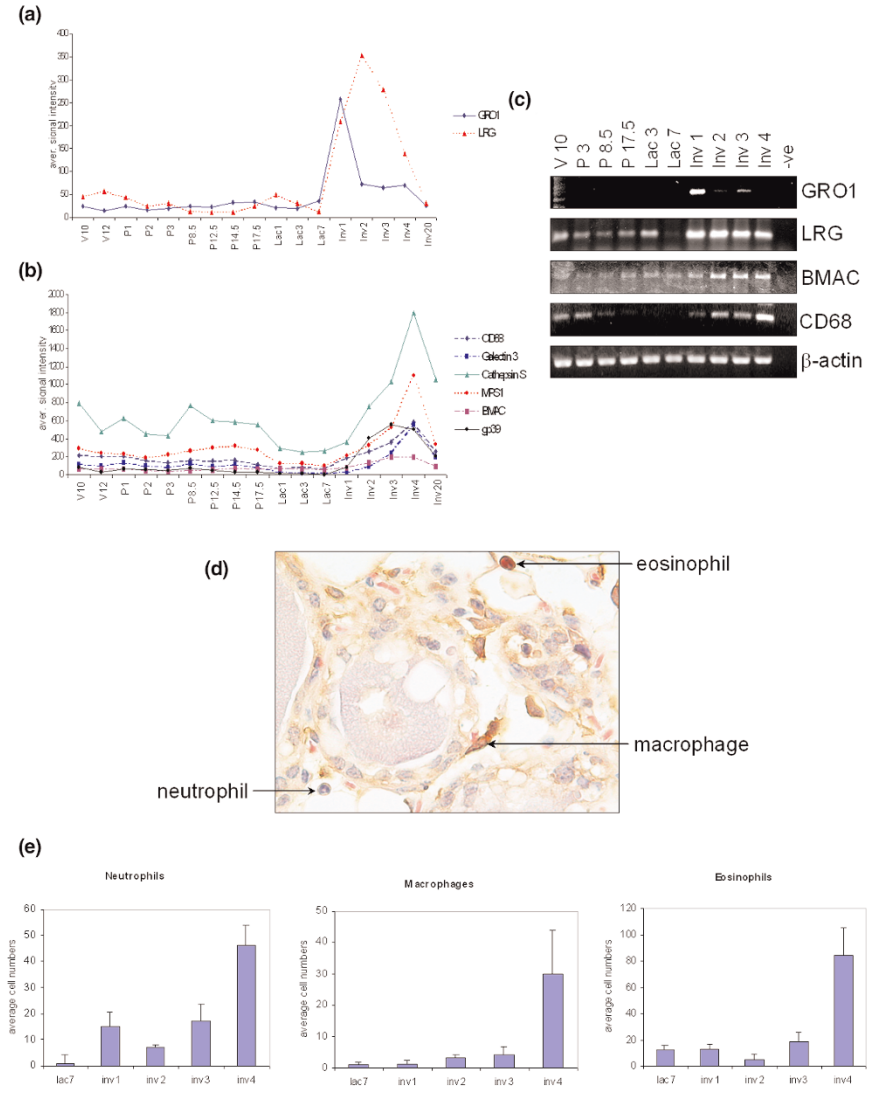

Activation of neutrophils, eosinophils and macrophages during involution. **(a)** RNA expression for *GRO1/IL-8/KC* and *LRG* derived from microarray analysis. **(b)** RNA expression for *BMAC*, *gp39*, *cathepsin S*, *MPS1*, *galectin 3* and *CD68* derived from microarray analysis. The *x*-axes of both graphs describe the different developmental stages: virgin (V10, V12), pregnancy (P1, P2, P3, P8.5, P12.5, P14.5, P17.5), lactation (Lac1, Lac3, Lac7) and involution (Inv1, Inv2, Inv3, Inv4, Inv20). The *y*-axes describe the averaged scaled signal of the triplicate samples for each time point. The intensity data for *LRG* have been scaled down 10-fold for display. **(c)** Semi-quantitative RT–PCR for *GRO1*, *LRG*, *BMAC* and *CD68* from a fourth independently collected RNA sample. **(d)** Identification of macrophages, neutrophils and eosinophils. The figure shows the immunohistochemical staining of a paraffin-embedded tissue section from a mouse mammary gland after 4 days of involution. Macrophages were identified by staining with F4/80 antibody and by their nuclear and cellular shapes. Eosinophils were identified by cross-reaction with the F4/80 antibody, polymorphonuclear structure and eosin staining. Neutrophils were identified through their polymorphonuclear structure, clear cytoplasm, slight eosin staining and non-staining with the F4/80 antibody. **(e)** Cell counts of neutrophils, eosinophils and macrophages present in the mammary tissue during involution. Tissue sections were stained with an antibody against F4/80 and counterstained with H&E; neutrophils and macrophages were counted. Cell counts were taken from 20 (neutrophils and eosinophils) and 50 (macrophages) high-power fields, respectively, from each section in triplicate from three individual mice.

anti-bacterial gene *single WAP-motif protein 2* (*SWAM2*) also showed a strong increase in its expression on the very first day of forced involution, but was not included in our list because it was also expressed during mid-pregnancy to late pregnancy.

LBP and CD14 proteins are expressed early during involution in the absence of infections

The upregulation of *LBP* was surprising because *LBP* function had so far been limited to LPS binding and its site of synthesis mainly to hepatocytes. We therefore wished

Table 4

List of acute-phase response-inducible and lipopolysaccharide-inducible proteins

Gene name	Genbank accession no.	Function	Cluster	References
APRF/STAT3	U08378	Transcription factor	8	[15,16]
C/EBPδ	X61800	Transcription factor	1	[21]
LPS-induced TNF-α factor, LITAF	AI852632	Transcription factor	8	[61]
CD14	X13333	LPS receptor	8	[26]
LBP	X99347	LPS-binding protein	8	[18]
Serum amyloid A2	M13521	Acute-phase response	8	[62]
Serum amyloid A3	X03505	Acute-phase response	1	[62]
Serum amyloid pseudogene	M17790	Acute-phase response?	8	[62]
α_1-acid glycoprotein 2	M12566	Acute-phase response	3	[63]
Caeruloplasmin	U49430	Acute-phase response	8	[64]
Secretory leukoprotease inhibitor	AF002719	Protease inhibitor	8	[36]
Immediate early response 3 (DIF2)	X67644	Immediate early response	8	[65]

LPS, lipopolysaccharide.

to confirm LBP expression in the mammary gland by other means. We extracted protein from mouse mammary glands from all stages of development and performed a Western blot analysis. This blot showed a strong increase in the amount of LBP in the mammary gland on the first day of involution, accompanied by a strong increase in the expression of CD14 protein (Fig. 5a). To ensure that this was not purely a consequence of a bacterial infection, we examined formalin-fixed paraffin-embedded tissue sections from lactation and early involution for the presence of pathogens by Gram staining. Neither Gram-negative nor Gram-positive bacteria could be detected in any of the samples analysed (data not shown).

CD14 is expressed in the luminal epithelial cells of the mouse mammary gland

CD14 is a known monocyte marker protein and is strongly involved in the phagocytosis of apoptotic cells by macrophages. Because luminal epithelial cells are involved in the phagocytosis of neighbouring apoptotic mammary epithelial cells during involution, we wished to know whether CD14 was also expressed in the luminal epithelium. We therefore performed IHC with a CD14-specific antibody. This revealed a strong increase in CD14 expression in the luminal epithelial cells at day 1 of involution, but not in the stroma (Fig. 5b). Unfortunately, LBP could not be detected by IHC either in paraffin-embedded or frozen mammary gland tissue, or in mouse liver sections with any antibody tested (data not shown).

Discussion

Involution of the mammary gland comprises a very complex and highly regulated cascade of programmed cell death and remodelling. It is believed to occur in two stages [3]: first, a reversible phase, lasting for about 2 days and characterised by an increased rate of apoptosis, and second, an irreversible remodelling phase that starts on the third day after forced weaning. To determine which genes are specifically expressed during the first 4 days of involution, we performed an oligonucleotide-microarray analysis over the pregnancy cycle of an adult mouse. We identified 145 genes that were specifically upregulated after removal of the pups, and obtained a comprehensive picture of the transcript changes that occur specifically during the first 4 days after forced weaning. Many of the genes identified have not previously been linked to involution. Our data imply that forced weaning in mice introduces an immune response in the mammary gland similar to that seen in wound repair. These data are in general agreement with the data published in this issue by Clarkson and colleagues [7], who used a different mouse system and a different analytical approach.

The APR pathway is activated during involution

The APR represents the first defence mechanism against disease and is part of the innate immune system, aimed at minimising tissue damage while enhancing repair processes [8]. After injury or infection, acute-phase protein expression is usually stimulated in the liver by the release of cytokines such as interleukin-1 (IL-1), interleukin-6 (IL-6) and tumour necrosis factor-α (TNF-α) from macrophages and monocytes at the sites of the trauma [9–11]. We identified 12 genes that were upregulated during the first 3 days of involution that either could be directly linked to the APR pathway or can in general be

Figure 5

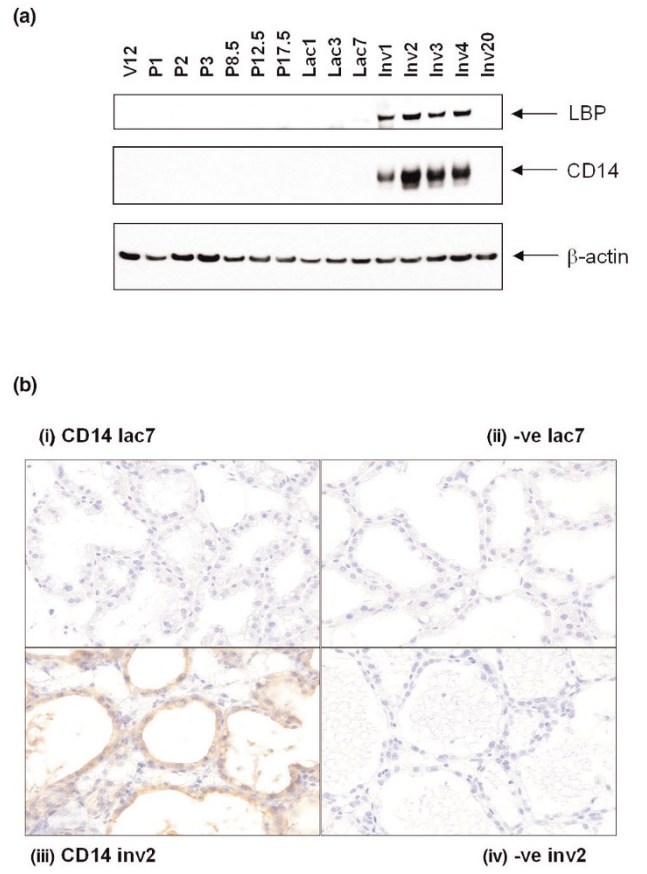

LBP and CD14 expression in the mouse mammary gland. **(a)** Western blot for LBP and CD14. Protein extracts from mouse mammary glands from the developmental stages virgin 12 weeks, pregnancy days 1, 2, 3, 8.5, 12.5 and 17.5, lactation days 1, 3 and 7, and involution days 1, 2, 3, 4 and 20 were separated on a denaturing gel; Western blotting was performed with anti-LBP, anti-CD14 and anti-β-actin antibodies. **(b)** Localisation of CD14 protein by immunohistochemistry. Paraffin-embedded sections from 7 days lactating **(i, ii)** and 2 days involuting **(iii, iv)** mouse mammary glands were stained with an anti-CD14-specific antibody. Negative controls contained no primary antibody.

activated by LPS, suggesting an important role for the APR pathway in involution. The finding that treatment of a mouse mammary gland with endotoxin leads not only to an increased resistance to staphylococcal mastitis but also to an accelerated involution of the gland itself [12] supports our hypothesis and suggests that a LPS-inducible immune response could be directly involved in the involution process. Our data also show that acute-phase proteins can be expressed in the mammary gland and do not act exclusively in a systemic way, or only during bacterial infection.

One of the genes identified encoded the transcription factor and key regulator of mammary gland involution STAT3 [13,14], which is also known as acute-phase response factor APRF [15,16]. Our data imply that a main function of STAT3 during this developmental stage might be the activation of this pathway. During an APR, STAT3 activates the genes *α_2-macroglobulin* [17], *LBP* [18] and *C/EBPδ* [19]. C/EBPδ is also involved in the activation of *LBP* after IL-6 signalling in hepatocytes [18] and of the genes *α_1-acid glycoprotein* [20] and *serum amyloid A* [21], and activates *CD14* transcription in transient transfection assays [22]. All these genes, with the exception of *α_2-macroglobulin*, which was undetectable in our study, were upregulated on the first day after forced weaning. However, their function during mammary gland involution is not yet clear. LBP activity has previously only been linked to the presentation of LPS to the LPS receptor CD14 during infection, whereas CD14 itself has also been linked to the phagocytosis of apoptotic cells [23]. The latter is commonly found on monocytes and macrophages [24,25] and on circulating polymorphonuclear neutrophil leukocytes in cattle [26], but can also be expressed by MCF7 cells in culture [27].

It has previously been shown that during involution apoptotic cells are phagocytosed not only by macrophages but also directly by their neighbouring epithelial cells [28–30]. We have now shown that CD14 is also expressed *in vivo* in the luminal epithelial cells during involution, suggesting that it might also be involved in the phagocytosis of apoptotic cells by surviving epithelial cells. Unfortunately, to our knowledge there are no antibodies available against LBP that could be successfully used for localisation studies. Although CD14-dependent apoptotic cell clearance by macrophages in cell culture does not seem to require LBP [31], this has not been demonstrated *in vivo* and might not be true for phagocytosis by mammary epithelial cells. Our finding that the transcript and protein level of LBP increased in parallel to CD14 at the onset of involution and in the absence of any bacterial infection suggests that LBP might also be involved in this important process. Since *LBP* is a downstream target of STAT3, and *CD14* can be activated by C/EBPδ, one function of *STAT3* as APR factor might be to enhance phagocytosis through the activation of *C/EBPδ* and hence *LBP*, to clear apoptotic cells from the mammary gland.

In contrast with bacterial infections, in which CD14-dependent phagocytosis through macrophages leads to the secretion of TNF-α and to inflammation [32], this is actively suppressed when macrophages phagocytose apoptotic cells [23,33]. The mechanism behind this phenomenon is not yet fully understood. At least three of our identified APR genes, *α_1-acid glycoprotein 2*, *caeruloplasmin* and *SLPI*, were upregulated on the first day after forced weaning and have been shown to modulate the activity of the immune system negatively during the acute-phase reaction, protecting cells from endotoxic shock [34–36]. They are therefore potential candidates for the active suppression of inflammation during involution.

During an APR, STAT3 is rapidly activated by tyrosine phosphorylation in response to IL-5, IL-6, epidermal growth factor, leukaemia inhibitory factor (LIF), oncostatin M (OSM), IL-11 and ciliary neurotrophic factor [37]. However, it is still controversial how STAT3 becomes activated during mammary gland involution. Hutt and DeWille [38] demonstrated that the IL-6 type cytokine OSM inhibits the growth of HC11 mouse mammary epithelial cells via a phospho-STAT3-dependent pathway and C/EBPδ. In addition, treatment of non-malignant human breast epithelial cells with OSM or LIF can inhibit proliferation [39]. Recently, LIF has been shown to participate in mouse mammary gland involution and to induce apoptosis in mammary epithelial cells [40]. In our study, the RNA level of the OSM receptor (OSMR) increased more than 10-fold specifically during the first 3 days of involution, supporting the view that OSM has a role during involution. Unfortunately, there was no probe for *OSM* on the array. In contrast, Kritikou and colleagues [41] recently found that the LIF receptor *LIFR* was upregulated 72 hours after forced weaning and that $LIF^{-/-}$ mice showed no phosphorylation of STAT3, indicating that STAT3 signalling during mammary gland involution was LIF-specific. However, the status of *OSM* in $LIF^{-/-}$ mice has not been shown, and because *OSM* and *LIF* are linked very closely on chromosome 11 it might be possible that *OSM* expression has also been directly or indirectly affected in the $LIF^{-/-}$ mice.

Thus, our data suggest a major role for the APR during the first days of mouse mammary gland involution, with possible roles in phagocytosis of apoptotic cells and the suppression of inflammation, and that OSM might have a role in the activation of the APR factor STAT3.

Gene expression profiles point to an early neutrophil response during involution

Although the early presence of neutrophils and the late presence of macrophages have been reported in the involution secretions of many species, including pigs, guinea pigs, sheep and cows [42–45], the same has not been reported for rats, humans or mice [30]. Our gene expression data strongly support a role for these cells during mouse mammary gland involution because the neutrophil-specific chemokine *GRO1/CXCL1* was specifically upregulated fivefold on the first day of involution, and the neutrophilic-granulocyte marker *LRG* [46] was upregulated most strongly on day 2 after forced weaning (Fig. 4a,c). This was confirmed by an elevated number of neutrophils (Fig. 4e) that infiltrated the mammary tissue after forced weaning, a response similar to that found in a healing wound [47]. However, whereas the transcript of *LRG* peaks on the second day after weaning, cell numbers decreased again slightly before increasing again on days 3 and 4. The elevated RNA level therefore reflects not only the influx of neutrophils into the mammary gland but also a transcriptional activation or RNA stabilisation of *LRG*. It is of interest to note that during days 1 and 2 after weaning, neutrophils were mainly localised in the blood vessels, whereas they were found mainly in the mammary tissue during days 3 and 4 (data not shown).

GRO1/CXCL1 is the murine functional orthologue of the human *interleukin 8* (*IL-8*) [48]. It is expressed in macrophages but the level of expression is reduced after phagocytosis of apoptotic cells [33]. On injury or during an inflammatory response it is also expressed in various epithelial cells [49–52] before many other chemokines [47,53,54]. It has an important role in wound healing [47], is maximally expressed 1 day after injury in a superficial woundbed and is spatially and temporally associated with neutrophil infiltration [47]. Because GRO1/CXCL1 can also be expressed in mammary epithelial cells [55], and LPS–CD14 complexes have been found to bind to Toll-like receptors on endothelial and epithelial cells, causing the release of IL-8 [56], it would be of interest to learn whether CD14 binding to apoptotic cells during mammary gland involution could induce GRO1/CXCL1 secretion from the mouse mammary epithelium.

Genes for macrophage differentiation suggest a secondary macrophage infiltration

Macrophages not only have an important role in the host defence mechanism but also function in normal tissue development and in postnatal mammary gland development [57]. Mice that carry a null mutation in the gene for the major growth factor for macrophages, *CSF1*, have a depleted population of macrophages in the mammary glands, leading to an impaired branching morphology [57]. Macrophages are also strongly involved in the clearance of apoptotic cells from the involuting mammary gland [28] and macrophage-specific genes have been found to be upregulated 7 days after forced weaning [6], whereas an increase in macrophage cell number has been reported from day 3 onwards [3]. The latter finding could be confirmed by using an F4/80 antibody, with macrophage numbers inside the mammary tissue clearly increasing on day 4 of involution, whereas the number of macrophages localised in the surrounding connective tissue already increased on day 3 (data not shown).

Interestingly, there was a marked increase in the number of eosinophils parallel to the increase of macrophages in the involuting tissue. Eosinophils, together with macrophages, are important for postnatal mammary gland development [57], and mice that are negative for eotaxin, a major eosinophilic chemo-attractant, show reduced branching and development of terminal end buds [57]. However, their specific function during mammary gland development is still unknown. Our data have now shown that eosinophils are present not only in the postnatal mammary gland but also in increasing

amounts in the involuting mammary gland, and that this increase was paralleled by a slightly elevated amount of eotaxin mRNA (data not shown). This points to an additional biological function of eosinophils in the mouse mammary gland distinct from any allergic response or defence against parasites.

Although we found a slight increase in the RNA levels of both *CSF1* and its receptor, *CSFR1*, which paralleled the expression of the other macrophage specific genes, these genes were also upregulated in virgin mice and during early pregnancy and are therefore not specific to involution. Instead, we found that the macrophage-attracting chemokine gene *CXCL14*/*BMAC*, the mouse orthologue of human *BRAK*, was increasingly expressed 3–4 days after involution was initiated, as were five genes associated with macrophage differentiation (Fig. 4b,c). In parallel, we found an increase in the number of macrophages 3 days after forced weaning (Fig. 4e). *CXCL14*/*BMAC* is expressed in several tissues including breast [58], and BRAK is secreted by fibroblasts and various epithelia to attract $CD14^+$ monocytes to sites of inflammation [59], where they differentiate into macrophages. CXCL14/BMAC is therefore a candidate signal for monocyte migration into the mammary gland during involution. These results again show that macrophages are not induced immediately after forced weaning but as a secondary response, after the activation of neutrophil-attracting and APR genes on the first day of involution. Figure 6 shows a hypothetical model of how phagocytosis might lead to a primary neutrophil activation, followed by secondary monocyte/macrophage activation.

Figure 6

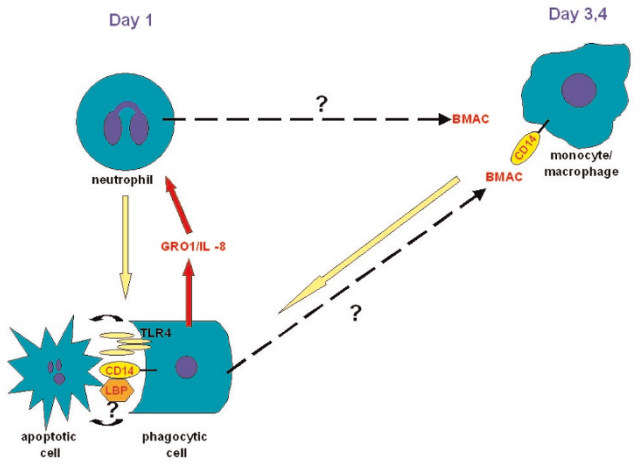

Model for early neutrophil and late macrophage activation. Apoptotic cells are recognised and phagocytosed by their neighbouring epithelial cells or professional and semi-professional cells (curved black arrows). This recognition and/or phagocytosis might involve LBP, CD14, signalling down by means of the Toll-like receptor 4 (TLR4). Activation of this receptor could lead to secretion of the neutrophil-attracting chemokine GRO1/IL-8 (red arrow) and to the attraction of neutrophils to the area of trauma (yellow arrow). This is followed by secretion of the $CD14^+$-monocyte-attracting chemokine BMAC (broken arrow), which could lead to monocyte infiltration on days 3 and 4 of involution (yellow arrow); monocytes would subsequently differentiate into macrophages.

Plasma cell numbers increase during involution

The largest group of genes upregulated during involution belonged to the immunoglobulin family. This increase was paralleled by an increased number of plasma cells in the tissue (Fig. 3b), suggesting that the elevated immunoglobulin RNA levels are due to an influx of plasma cells into the mammary tissue, rather than only a transcriptional activation. This is in agreement with an increase in plasma cell number late during the dry period of an uninfected bovine mammary gland [60]. However, whereas in cattle the expression of immunoglobulins increases further until very late in involution [60], the same was not seen in mice. Instead, RNA expression decreased again towards day 20 after forced weaning. Immunoglobulins in the involuting mammary gland are believed to opsonise bacteria and to act as antitoxins, when the possibility of infection is greatest immediately after weaning. Whether the increase could also reflect an immune response towards the vast amount of cell death in the tissue is still open to speculation. It has been shown that macrophages that phagocytose apoptotic cells degrade them completely and are incapable of antigen presentation to T-cells, and that there is therefore no specific, antibody-mediated immune response to self-antigens during mammary involution [30]. However, this is still controversial [29].

Conclusion

Our work has shown that microarray analysis can be used to characterise a complex developmental system and the processes that occur during the different stages, and to identify genes that are involved in the early stages of mouse mammary gland involution. Although the physiological significance of many newly identified genes in the involution process still has to be verified, our study has, together with the accompanied publication in this issue by Clarkson and colleagues [7], for the first time given a comprehensive picture of the transcriptional changes that occur during this very important developmental process. At the same time it has posed many new questions and formed a base on which to build future work. In particular, the main function of *STAT3*/*APRF* during involution still remains to be resolved. Transcriptome analysis of a conditional STAT3-null mouse after forced weaning should give us valuable insight into the pathways induced by STAT3 during mammary gland involution. It would also be of significant importance to learn whether mammary glands from *LBP* or *CD14* knockout mice showed any signs of delayed phagocytosis or involution.

Additional files

The following Additional files are available online:

Additional file 1
A tab-delimited text file containing a table of the normalised signal data from all 12488 probe sets and 17 time points of mouse mammary gland development in triplicate (A, B, and C). It further contains the detection calls and averaged signal data, plus an annotation table retrieved from the NetAffx-website, including probe set ID, name of chip used, gene titles, gene symbols, Genbank accession numbers, sequence descriptions, Unigene ID, SwissProt ID, and full-length reference sequence accession numbers.
See http://breast-cancer-research.com/content/supplementary/bcr753-S1.txt

Additional file 2
A tab-delimited text file containing a table of those genes which were specifically up or down regulated during involution, including the normalised signal data from 17 time points of mouse mammary gland development in triplicate (A, B, and C), probe set ID, gene symbols and gene titles.
See http://breast-cancer-research.com/content/supplementary/bcr753-S2.txt

Competing interests

None declared.

Acknowledgements

The project was run in close collaboration with Affymetrix UK. We thank Affymetrix UK for their financial and technical support. We also thank Professor JW Pollard for the kind gift of the F4/80 antibody; Dr Catriona Young and Dr Giorgia Riboldi-Tunnicliffe from the SHWFGF at Glasgow University for their technical help; Dr Christine Watson, Dr Richard Clarkson and Dr David Stott for critical helpful discussions; and Professor Chris Knight from the Hannah Research Institute, Ayr, UK, whose intellectual input into this work was crucial to the successful outcome of the project. The work was supported by a Breakthrough Breast Cancer programme grant (to BG).

References

1. Richert MM, Schwertfeger KL, Ryder JW, Anderson SM: **An atlas of mouse mammary gland development.** *J Mammary Gland Biol Neoplasia* 2000, **5:**227-241.
2. Masso-Welch PA, Darcy KM, Stangle-Castor NC, Ip MM: **A developmental atlas of rat mammary gland histology.** *J Mammary Gland Biol Neoplasia* 2000, **5:**165-185.
3. Lund LR, Romer J, Thomasset N, Solberg H, Pyke C, Bissell MJ, Dano K, Werb Z: **Two distinct phases of apoptosis in mammary gland involution: proteinase-independent and -dependent pathways.** *Development* 1996, **122:**181-193.
4. Li M, Liu X, Robinson G, Bar-Paled U, Wagner K-U, Young WS, Hennighausen L, Furth PA: **Mammary derived signals activate programmed cell during the involuting mammary gland.** *Proc Natl Acad Sci USA* 1997, **94:**3425-3430.
5. Marti A, Lazar H, Ritter P, Jaggi R: **Transcription factor activities and gene expression during mouse mammary gland involution.** *J Mammary Gland Biol Neoplasia* 1999, **4:**145-152.
6. Master SR, Hartman JL, D'Cruz CM, Moody SE, Keiper EA, Ha SI, Cox JD, Belka GK, Chodosh LA: **Functional microarray analysis of mammary organogenesis reveals a developmental role in adaptive thermogenesis.** *Mol Endocrinol* 2000, **16:**1185-1203.
7. Clarkson RWE, Wayland MT, Lee J, Freeman T, Watson CJ: **Gene expression profiling of mammary gland development reveals putative roles for death receptors and immune mediators in post-lactational regression.** *Breast Cancer Res* 2004, **6:**R92-R109.
8. Eckersall PD: **Recent advances and future prospects for the use of acute phase proteins as markers of disease in animals.** *Revue Méd Vét* 2000, **151:**577-584.
9. Dinarello CA: **Interleukin-1 and the pathogenesis of the acute phase response.** *New Engl J Med* 1984, **311:**1413-1418.
10. Heinrich PC, Castell JC, Andus T: **Interleukin-6 and the acute phase response.** *Biochem J* 1990, **265:**621-636.
11. Beutler B, Cerami A: **Cachectin/tumor necrosis factor: an endogenous mediator of shock and inflammation.** *Immunol Res* 1986, **5:**281-293.
12. Anderson JC: **The increased resistance of mice to experimental staphylococcal mastitis following inoculation of endotoxin.** *Res Vet Sci* 1976, **21:**64-68.
13. Chapman RS, Lourenco PC, Tonner E, Flint DJ, Selbert S, Takeda K, Akira S, Clarke AR, Watson CJ: **Suppression of epithelial apoptosis and delayed mammary gland involution in mice with a conditional knockout of Stat3.** *Genes Dev* 1999, **13:** 2604-2616.
14. Humphreys RC, Bierie B, Zhao L, Raz R, Levy D, Hennighausen L: **Deletion of Stat3 blocks mammary gland involution and extends functional competence of the secretory epithelium in the absence of lactogenic stimuli.** *Endocrinology* 2002, **143:** 3641-3650.
15. Akira S, Nishio Y, Inoue M, Wang XJ, Wei S, Matsusaka T, Yoshida K, Sudo T, Naruta M, Kishimoto T: **Molecular cloning of APRF, a novel IFN-stimulated gene factor 3 p91-related transcription factor involved in the gp130-mediated signaling pathway.** *Cell* 1994, **77:**63-71.
16. Zhong Z, Wen Z, Darnell JE: **Stat3: a new family member that is activated through tyrosine phosphorylation in response to EGF and IL-6.** *Science* 1994, **264:**95-98.
17. Trautwein C, Rakemann T, Niehof M, Rose-John S, Manns MP: **Acute-phase response factor, increased binding, and target gene transcription during liver regeneration.** *Gastroenterology* 1996, **110:**1854-1862.
18. Schumann RR, Kirschning CJ, Unbehaun A, Aberle HP, Knope HP, Lamping N, Ulevitch RJ, Herrmann F: **The lipopolysaccharide-binding protein is a secretory class 1 acute-phase protein whose gene is transcriptionally activated by APRF/STAT-3 and other cytokine-inducible nuclear proteins.** *Mol Cell Biol* 1996, **16:**3490-3503.
19. Cantwell CA, Sterneck E, Johnson PF: **Interleukin-6-specific activation of the C/EBPdelta gene in hepatocytes is mediated by Stat3 and Sp1.** *Mol Cell Biol* 1998, **18:**2108-2117.
20. Boudreau F, Yu SJ, Asselin C: **CCAAT/enhancer binding proteins beta and delta regulate alpha1-acid glycoprotein gene expression in rat intestinal epithelial cells.** *DNA Cell Biol* 1998, **17:**669-677.
21. Alam T, An MR, Papaconstantinou J: **Differential expression of three C/EBP isoforms in multiple tissues during the acute phase response.** *J Biol Chem* 1992, **267:**5021-5024.
22. Pan Z, Hetherington CJ, Zhang DE: **CCAAT/enhancer-binding protein activates the CD14 promoter and mediates transforming growth factor beta signaling in monocyte development.** *J Biol Chem* 1999, **274:**23242-23248.
23. Devitt A, Moffa, OD, Raykundalia C, Capra JD, Simmons DL, Gregory CD: **Human CD14 mediates recognition and phagocytosis of apoptotic cells.** *Nature* 1998, **392:**505-509.
24. Wright SD: **CD14: a leukocyte membrane protein that functions in the response to endotoxin [abstract].** *FASEB J* 1990, **4:**A1848.
25. Wright SD, Ramos RA, Tobias PS, Ulevitch RJ, Mathison JC: **CD14, a receptor for complexes of lipopolysaccharide (LPS) and LPS binding protein.** *Science* 1990, **249:**1431-1433.
26. Paape MJ, Lillius EM, Wiitanen PA, Kontio MP: **Intramammary defense against infections induced by *Escherichia coli* in cows.** *Am J Vet Res* 1996, **57:**477-482.
27. Labeta MO, Vidal K, Nores JE, Arias M, Vita N, Morgan BP, Guillemot JC, Loyaux D, Ferrara P, Schmid D, Affolter M, Borysiewicz

LK, Donnet-Hughes A, Schiffrin EJ: **Innate recognition of bacteria in human milk is mediated by a milk-derived highly expressed pattern recognition receptor, soluble CD14.** *J Exp Med* 2000, **191:**1807-1812.
28. Walker NI, Bennett RE, Kerr JFR: **Cell death by apoptosis during involution of the lactating breast in mice and rats.** *Am J Anat* 1989, **185:**19-32.
29. Fadok VA: **Clearance: the last and often forgotten stage of apoptosis.** *J Mammary Gland Biol Neoplasia* 1999, **4:**203-211.
30. Monks J, Geske FJ, Lehman L, Fadok VA: **Do inflammatory cells participate in mammary gland involution?** *J Mammary Gland Biol Neoplasia* 2002, **7:**163-176.
31. Gregory CD: **CD14-dependent clearance of apoptotic cells: relevance to the immune system.** *Curr Opin Immunol* 2000, **12:** 27-34.
32. Old LJ: **Tumor necrosis factor.** *Sci Am* 1988, **258:**59-75.
33. Fadok VA, Bratton DL, Konowal A, Freed PW, Westcott JY, Henson PM: **Macrophages that have ingested apoptotic cells in vitro inhibit proinflammatory cytokine production through autocrine/paracrinemechanisms involving TGFβ, PGE2, and PAF.** *J Clin Invest* 1998, **1001:**890-898.
34. Laurent PE: **Clinical measurement of acute phase proteins to detect and monitor infectious disease.** In *Acute Phase Proteins in the Acute Phase Response*. Edited by Pepys MB. New York: Springer-Verlag; 1989:151-159.
35. Jin FY, Nathan C, Radzioch D, Ding A: **Secretory leukocyte protease inhibitor: a macrophage product induced by and antagonistic to bacterial lipopolysaccharide.** *Cell* 1997, **88:**417-426.
36. Zhu J, Nathan C, Jin W, Sim D, Ashcroft GS, Wahl SM, Lacomis L, Erdjument-Bromage H, Tempst P, Wright CD, Ding A: **Conversion of proepithelin to epithelins. Roles of SLPI and elastase in host defense and wound repair.** *Cell* 2002, **111:**867-878.
37. Lutticken C, Wegenka UM, Yuan J, Buschmann J, Schindler C, Ziemiecki A, Harpur AG, Wilks AF, Yasukawa K, Taga T: **Association of transcription factor APRF and protein kinase Jak1 with the interleukin-6 signal transducer gp130.** *Science* 1994, **263:** 89-92.
38. Hutt JA, DeWille JW: **Oncostatin M induces growth arrest of mammary epithelium via a CCAAT/enhancer-binding protein delta-dependent pathway.** *Mol Cancer Ther* 2002, **1:**601-610.
39. Grant SL, Douglas AM, Goss GA, Begley CG: **Oncostatin M and leukemia inhibitory factor regulate the growth of normal human breast epithelial cells.** *Growth Factors* 2001, **19:**153-162.
40. Schere-Levy C, Buggiano V, Quaglino A, Gattelli A, Cirio, MC, Piazzon I, Vanzulli S, Kordon EC: **Leukemia inhibitory factor induces apoptosis of the mammary epithelial cells and participates in mouse mammary gland involution.** *Exp Cell Res* 2003, **282:**35-47.
41. Kritikou EA, Sharkey A, Abell K, Came PJ, Anderson E, Clarkson RWE, Watson CJ: **A dual, non-redundant, role for LIF as a regulator of development and STAT3-mediated cell death in mammary gland.** *Development* 2003, **130:**3459-3468.
42. Lee CS, McDowell GH, Lascelles AK: **The importance of macrophages in the removal of fat from the involuting mammary gland.** *Res Vet Sci* 1969, **10:**34-38.
43. Nordin W, Lee CS: **Cytology of milk in guinea pigs.** *Acta Anat* 1982, **113:**135-144.
44. Lee CS, McCauley I, Hartmann PE: **Light and electron microscopy of cells in pig colostrum, milk and involution secretion.** *Acta Anat* 1983, **116:**126-135.
45. Colditz IG**: Studies on the inflammatory response during involution of the ovine mammary gland.** *Q J Exp Physiol* 1988, **73:** 363-368.
46. O'Donnell LC, Druhan LJ, Avalos BR: **Molecular characterization and expression analysis of leucine-rich alpha2-glycoprotein, a novel marker of granulocytic differentiation.** *J Leukoc Biol* 2002, **72:**478-485.
47. Engelhardt E, Toksoy A, Goebeler M, Debus S, Brocker EB, Gillitzer R: **Chemokines IL-8, GROalpha, MCP-1, IP-10, and Mig are sequentially and differentially expressed during phase-specific infiltration of leukocyte subsets in human wound healing.** *Am J Pathol* 1998, **153:**1849-1860.
48. Wiekowski MT, Chen SC, Zalamea P, Wilburn BP, Kinsley DJ, Sharif WW, Jensen KK, Hedrick JA, Manfra D, Lira SA: **Disruption of neutrophil migration in a conditional transgenic model: evidence for CXCR2 desensitization in vivo.** *J Immunol* 2001, **167:** 7102-7110.
49. Aubry F, Habasque C, Satie AP, Jegou B, Samson M: **Expression and regulation of the CXC-chemokines, GRO/KC and IP-10/mob-1 in rat seminiferous tubules.** *Eur Cytokine Netw* 2000, **11:**690-698.
50. Heeckeren A, Walenga R, Konstan MW, Bonfield T, Davis PB, Ferkol T: **Excessive inflammatory response of cystic fibrosis mice to bronchopulmonary infection with *Pseudomonas aeruginosa*.** *J Clin Invest* 1997, **100:**2810-2815.
51. Jones CE, Chan K: **Interleukin-17 stimulates the expression of interleukin-8, growth-related oncogene-alpha, and granulocyte-colony-stimulating factor by human airway epithelial cells.** *Am J Respir Cell Mol Biol* 2002, **26:**748-753.
52. Mehrad B, Strieter RM, Moore TA, Tsai WC, Lira SA, Standiford TJ: **CXC chemokine receptor-2 ligands are necessary components of neutrophil-mediated host defense in invasive pulmonary aspergillosis.** *J Immunol* 1999, **163:**6086-6094.
53. Endlich B, Armstrong D, Brodsky J, Novotny M, Hamilton TA: **Distinct temporal patterns of macrophage-inflammatory protein-2 and KC chemokine gene expression in surgical injury.** *J Immunol* 2002 **168:**3586-3594.
54. Rovai LE, Herschman HR, Smith JB: **The murine neutrophil-chemoattractant chemokines LIX, KC, and MIP-2 have distinct induction kinetics, tissue distributions, and tissue-specific sensitivities to glucocorticoid regulation in endotoxemia.** *J Leukoc Biol* 1998, **64:**494-502.
55. Anisowicz A, Zajchowski D, Stenman G, Sager R: **Functional diversity of GRO gene expression in human fibroblasts and mammary epithelial cells.** *Proc Nat Acad Sci USA* 1988, **85:** 9645-9649.
56. Paape M, Mehrzad J, Zhao J, Detilleux J, Burvenich C: **Defense of the bovine mammary gland by polymorphonuclear neutrophil leukocytes.** *J Mammary Gland Biol Neoplasia* 2002 **7:**109-121.
57. Gouon-Evans V, Rothenberg ME, Pollard JW: **Postnatal mammary gland development requires macrophages and eosinophils.** *Development* 2000, **127:**2269-2282.
58. Sleeman MA, Fraser JK, Murison JG, Kelly SL, Prestidge RL, Palmer DJ, Watson JD, Kumble KD: **B cell- and monocyte-activating chemokine (BMAC), a novel non-ELR alpha-chemokine.** *Int Immunol* 2000, **12:**677-689.
59. Kurth I, Willimann K, Schaerli P, Hunziker T, Clark-Lewis I, Moser B: **Monocyte selectivity and tissue localization suggests a role for breast and kidney-expressed chemokine (BRAK) in macrophage development.** *J Exp Med* 2001, **194:**855-861.
60. Nickerson SC: **Immunological aspects of mammary involution.** *J Dairy Sci* 1989, **72:**1665-1678.
61. Myokai F, Takashiba S, Lebo R, Amar S: **A novel lipopolysaccharide-induced transcription factor regulating tumor necrosis factor α gene expression: molecular cloning, sequencing, characterization, and chromosomal assignment.** *Proc Natl Acad Sci USA* 1999, **96:**4518-4523.
62. Kushner I, Mackiewicz A: **Acute phase proteins as disease markers.** *Dis Markers* 1987, **5:**1-11.
63. Hochepied T, Berger FG, Baumann H, Libert C: **α_1-acid glycoprotein: and acute phase protein with inflammatory and immunomodulating properties.** *Cyt Growth Factor Rev* 2003, **14:**25-34.
64. Gitlin JD: **Transcriptional regulation of ceruloplasmin gene expression during inflammation.** *J Biol Chem* 1988, **263:**6281-6287.
65. Pietzsch A, Buchler C, Aslanidis C, Schmitz G**: Identification and characterization of a novel monocyte/macrophage differentiation-dependent gene that is responsive to lipopolysaccharide, ceramide, and lysophosphatidylcholine.** *Biochem Biophys Res Commun* 1997, **235:**4-9.

Correspondence

Torsten Stein, Division of Cancer Sciences and Molecular Pathology, Western Infirmary, University of Glasgow, Glasgow G11 6NT, UK. Tel: +44 141 211 1942; fax: +44 141 337 2494; e-mail: ts33s@udcf.gla.ac.uk